Precise analysis and control of polymerization kinetics using a micro flow reactor

Asano, Shusaku
Department of Chemical Engineering, Kyoto University

Maki, Taisuke
Department of Chemical Engineering, Kyoto University

Nakayama, Ryutaro
Department of Chemical Engineering, Kyoto University

Utsunomiya, Ryuji
Department of Chemical Engineering, Kyoto University

他

出版情報：Chemical Engineering and Processing: Process Intensification. 119, pp.73-80, 2017-09-01. Elsevier
バージョン：
権利関係：

Title of the article

Precise analysis and control of polymerization kinetics using a micro flow reactor

Authors

Shusaku Asano[a], Taisuke Maki[a,*], Ryutaro Nakayama[a], Ryuji Utsunomiya[a], Yosuke Muranaka[a], Toshiharu Kuboyama[b] and Kazuhiro Mae[a]

[a]Department of Chemical Engineering, Kyoto University, Kyoto, Japan

[b]SUMITOMO BAKELITE CO., LTD., Tokyo, Japan

*) Corresponding author

Taisuke Maki

Department of Chemical Engineering, Kyoto University,

Kyoto-daigaku Katsura, Nishikyo-ku, Kyoto 615-8510 Japan

Tel.: +81-75-383-2688

E-mail: tmaki@cheme.kyoto-u.ac.jp

Abstract

Polymerization has a fast, complex reaction kinetics, which is difficult to control with conventional equipment. We employed a micro flow system to design ideal reaction conditions based on a kinetic model. Rate analysis was conducted at a wide range of reaction times, from 10 to 3600 s. The concentration profile of an active intermediate was estimated and utilized for designing advanced reaction schemes, which required rapid

concentration and temperature changes. A block copolymer of hexyl norbornene and norbornene carboxylic acid alkyl ester was synthesized by developing a sequential polymerization system. The temperature jump operation, with 0.5 s initiation at 60 °C followed by 30 s propagation at 0 °C, generated a hexyl norbornene polymer with a sharp molecular weight distribution.

Keywords: polymerization kinetics, norbornene, micro flow reactor

1. Introduction

A flow reactor with a small scale diameter, typically tens of microns to a millimeter, enables rapid mass and heat transfer via the short diffusion length, high surface to volume ratio and controlled secondary flows [1,2]. Therefore, a micro flow reactor is an attractive tool for producing fine chemicals and materials that require the strict control of process conditions for product quality [3,4]. For instance, monodispersed quantum dots were synthesized in a silicon carbide micro flow reactor with rapid heating [5]; a synthetic retinoid TAC-101 was synthesized via the Br/Li exchange reaction with rapid mixing [6]; and zeolitic imidazolate flamework-8 particles with controlled sizes, shapes and gate adsorption characteristics were produced using a micromixer with 10 sub-streams [7]. Continuous flow synthesis also improves reproducibility [8] and productivity [9]. Therefore, small sized flow reactors, which do not necessarily have a microscale, have been intensively applied for on-demand production, especially of active pharmaceutical ingredients [10–12].

Micro flow reactors have been employed for precision polymerization for decades [13]. First, rapid mixing and heat removal have a significant advantage to make a sharp molecular weight distribution by providing strict control of the concentration and temperature. For example, improvement of molecular weight distributions in the radical polymerization of styrene [14], cationic polymerization of vinyl ether [15], and Grignard metathesis polymerization of 3-hexylthiophene [16] have been reported. Smaller polymer particles with a tighter size distribution were generated in an ultrasound-assisted, surfactant-free emulsion polymerization in a narrow channel reactor coil [17]. A tiny reaction volume with pressure resistance has advantages that allow us to safely conduct an unconventional reaction scheme that involves hazardous chemicals and high

temperature and pressure. End group modification using trimethylsilyl azide at 120 °C and 20 bar, which would have explosion risks and the formation of extremely toxic HN_3 gasses in a batch reactor, was successfully achieved in a commercial microchip [18]. The flow system can be equipped with in-line purification and process automation, which dramatically improve productivity and scalability. A modular flow system with a membrane separator achieved sequence defined polymer synthesis with a 66 g day^{-1} throughput [19].

Almost all of the above polymerization studies with micro flow reactors have been empirically optimized by changing the temperature, residence time, concentrations and reactors, i.e., without kinetic modeling. One reason is probably the complexity of the polymerization mechanisms. However, optimization based on reaction kinetics would effectively improve the quality and productivity of the process. Kinetic modeling and micro flow reactors would have a strong synergy. Micro flow reactors can acquire reliable data for rate analysis by controlling the reaction time at a surprisingly high-resolution on the order of milliseconds [20]. Furthermore, the complicated behavior of secondary flows and concentration profile in a microreactor can be analyzed and optimized with the assistance of computational fluid dynamics simulation and 3D printing techniques [21]. An automated experiment that changes numerous variables is also possible with a compact system consisting of a micro flow reactor, pumps, and an analyzer [22]. Rapid heat and mass transfer enable us to realize the ideal conditions derived from the kinetic model, even if they require temperature changes within a second.

This study intended to invent a precision polymerization procedure based on polymerization kinetics. We chose the non-living coordination polymerization of norbornene derivatives as a model. Fig. 1 illustrates a proposed reaction mechanism for

this system based on Barnes et al. [23]. Polymerization proceeds via insertion and coordination of a monomer to the nickel complex. There are two types of termination via proton transfer to an end group norbornene, where one is in the state of one monomer coordination (termination 1) and the other one is in the state of two monomer coordination (termination 2). This study attempted to acquire the kinetic parameter for each step and design a procedure to synthesize a block copolymer and a polymer with a monodispersed molecular weight distribution. These are challenging objectives in a non-living system in which an undesirable termination reaction exists. However, it would be a promising approach to intensify the versatility of polymer processing by expanding the scope of precision polymerization.

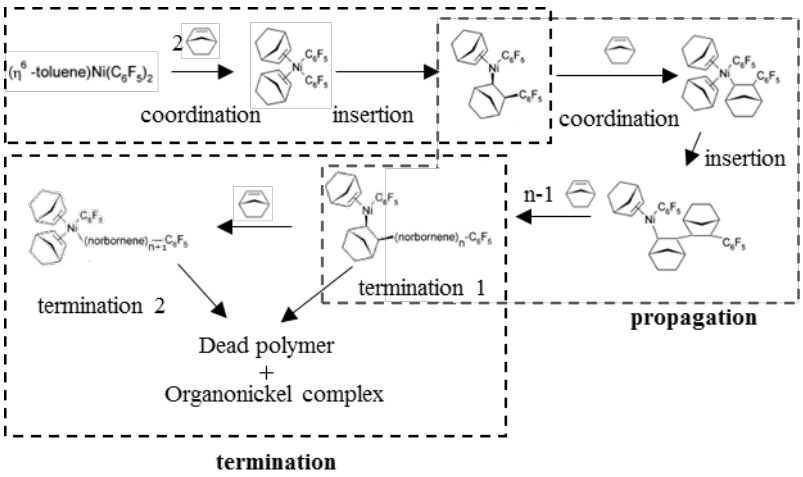

Fig. 1. Proposed reaction mechanism based on Barnes et al. [23]

2. Methods

2.1. Materials

Monomer materials of hexyl norbornene (monomer A) and norbornene carboxylic acid alkyl ester (monomer B) and an initiator of (η^6-tolunene)Ni(C_6F_5)$_2$ were supplied from SUMITOMO BAKELITE (Tokyo, Japan). Toluene, tetrahydrofuran (THF), ethyl acetate, 30 wt% hydrogen peroxide, and acetic acid were purchased from Wako Pure

Chemical Industries (Osaka, Japan). The monomer was diluted with a mixture of toluene and ethyl acetate at a weight ratio of 3:7. The prepared monomer solution was dried by bubbling with nitrogen gas for 30 minutes before usage. The initiator solution was prepared by diluting (η^6-tolunene)Ni(C_6F_5)$_2$ with toluene. The aqueous peracetic acid solution for termination was prepared as THF = 27 wt%, H_2O = 53 wt%, H_2O_2 = 8 wt%, and CH_3COOH = 12 wt%.

2.2. Constant temperature polymerization for kinetic analysis

Fig. 2(a) illustrates the reactor system. The reactor was constructed using SUS tubing and tees. Tubing with an outer diameter (o.d.) of 1/16" and an inner diameter (i.d.) of 1.0 mm was connected to union tees (Swagelok, USA) with an i.d. of 1.3 mm. All tubing was coiled to enhance the heat and mass transfer and to reduce the residence time distribution [24,25]. The first tee mixes the monomer and initiator solution, and the other tee injects the peracetic acid solution to terminate the reaction. All were placed in a water bath to keep the temperature constant. The reaction time was controlled by changing the flow rate and length of tubing between tees. Two meters of tubing was used for reaction times from 10 to 20 s, 5 m of tubing was used for 30 to 60 s, and 10 m of tubing was used for 150 to 3600 s. Four concentration sets were examined. The monomer A ([M]) and initiator ([I]) concentrations after the first tee for each set are listed as follows:

set 1 (monomer 5 wt%): [M] = 0.25 M, [I] = 0.0049 M

set 2 (monomer 10 wt%): [M] = 0.49 M, [I] = 0.0049 M

set 3 (monomer 15 wt%): [M] = 0.74 M, [I] = 0.0049 M

set 4 (monomer 14 wt%): [M] = 0.68 M, [I] = 0.0048 M.

The ratios of the flow rates of the monomer solution, 5 kg m^{-3} initiator solution, and terminator solution were 0.86 : 1 : 1 for set 4 and 1.3 : 1 : 1 for the other sets. The flow

rate was controlled using PHD Ultra syringe pumps (Harvard Apparatus, Massachusetts, USA).

To confirm that the kinetic parameters were not contaminated by heat and mass transfer issue, which originates from the enhanced viscosity with molecular weight build up, we measured the viscosity of a polymer solution. The sample polymer solution was obtained by polymerization in a batch reactor. Set 4 concentration was employed. A conical flask placed in a water bath at 25 °C was used as a batch reactor. Air was purged with nitrogen gas before the injection of initiator solution. After 1 h reaction, kinematic viscosity of the solution was measured by an Ostwald viscometer with an inner diameter of 1.75 mm (As One, Osaka, Japan). Terminator solution was not added for measuring the viscosity before the dilution. The density of the solution was also obtained by weighing the 1 mL solution to convert kinematic viscosity to absolute viscosity.

2.3. Block copolymer synthesis

Fig. 2(b) illustrates the reactor system. Union tees with an i.d. of 0.33 mm were used. The first tee mixes the monomer A and initiator solutions. The second tee mixes the reacting stream and the monomer B solution. The third tee injects the terminator. Two water baths were used to change the temperature from 40 °C to 25 °C. The lengths of tubing were 2 m for both the first and second steps. The concentrations after the first tee were [M] = 0.61 M and [I] = 0.0043 M. The concentration of monomer B was 0.825 M after the second tee. The residence times were 30 s and 15 s for the first and second steps, respectively. The flow rates were 0.85, 0.73, 1.58, and 3.16 mL min^{-1} for the monomer A solution, initiator solution (5 kg m^{-3}), monomer B solution, and terminator solution, respectively. All other conditions were the same as described in section 2.2. For the

control experiments, polymerization of monomer A alone with the first step and the block copolymer synthesis with twice the residence time (60 s for the 1st step and 30 s for the 2nd step) and with half the flow rate (0.43, 0.37, 0.79 and 1.08 mL min^{-1}) were conducted.

2.4. Homopolymer synthesis with temperature jump

Fig. 2(b) illustrates the reactor system. Of note, a 0.13 m length of tubing with an i.d. of 0.5 mm was used for the high temperature zone; a 2 m length of tubing with an i.d. of 1 mm was used for the low temperature zone. A water bath with a drilled screw hole was placed in a larger bath. Two tubes were connected at the drilled hole. The inner bath was kept at 60 °C by a heater. The outer bath was maintained at 0 °C with ice. The residence times were 0.5 s and 30 s for the low and high temperature zones, respectively. The flow rates were 1.44, 1.70, and 1.57 mL min^{-1} for the monomer A solution, initiator solution (30 kg m^{-3}), and terminator solution, respectively. The concentrations after the first tee were [M] = 1.0 M and [I] = 0.033 M. All other conditions were the same as those described in section 2.2. For a control experiment, constant temperature operations for a 0.5-s reaction time at 60 °C and for a 30-s reaction time at 0 °C were conducted by removing one of the tubes.

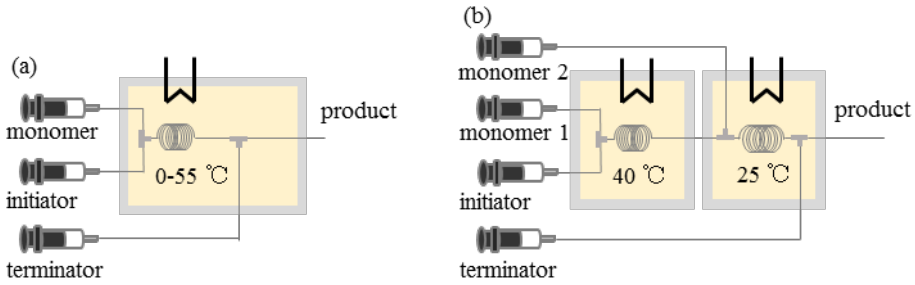

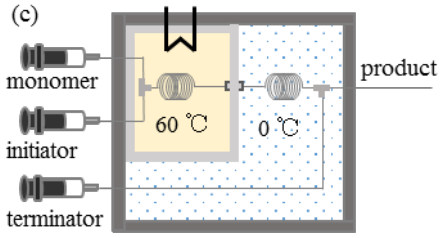

Fig. 2. Reactor setups: (a) constant temperature operation for kinetic analysis; (b) block copolymer synthesis; and (c) homopolymer synthesis with a temperature jump

2.5. Analysis

Conversion of the monomer was calculated from the monomer concentration in the solution after the reaction as determined by gas chromatography. A GC-2010 (Shimadzu, Kyoto, Japan) equipped with a flame ionization detector and a non-polar capillary column TC-1 (GL-Science, Tokyo, Japan) was used. Molecular weight distributions were obtained by high-performance liquid chromatography (HPLC). The separation column was a Shodex GPC LF-804 column (Showa Denko, Tokyo, Japan). A refractive index detector RID-6A (Shimadzu) and esa Corona charged aerosol detector (DIONEX, California, USA) combined with an SPD-20A UV detector (Shimadzu) were used as detection units. THF was used as the mobile phase with a 1 mL min^{-1} flow rate and was pumped with a LC10-ATvp HPLC pump (Shimadzu). Gradient polymer elution chromatography (GPEC) was conducted to analyze the composition and homogeneity of a copolymer. An Alliance 2695 HPLC system (Waters, Massachusetts, USA) equipped with a Luna C18(2) separation column (Phenomenex, California, USA) with a 2420 evaporative light scattering detector (Waters) was employed for GPEC. The flow rate of the mobile phase was fixed at 1 mL min^{-1}. A mixture of acetonitrile and THF was used as the mobile phase. The linear gradient was adapted, and the percentage of THF was changed from 40% to 100% over 7.5 min after 0.5 min of operation. The composition

was again changed from 100% to 40% over 0.5 min after 11 min of operation.

2.6. Parameter fitting

A kinetic model based on the mechanism in Fig. 1 was built as shown below.

Initiation	Coordination 1	$I + M \rightleftarrows R_0$	$r = k_{I1}[I][M] - k_{-I1}[R_0]$
	Coordination 2	$R_0 + M \rightleftarrows R_1$	$r = k_{I2}[R_0][M] - k_{-I2}[R_1]$
	Insertion	$R_1 \rightarrow P_1$	$r = k_{I3}[R_1]$
Propagation	Coordination	$P_n^* + M \rightleftarrows R_{n+1}$	$r = k_M[P_n^*][M] - k_{-M}[R_{n+1}]$
	Insertion	$R_n \rightarrow P_n^*$	$r = k_P[R_n]$
Termination	Termination 1	$P_n^* \rightarrow P_n$	$r = k_{T1}[P_n^*]$
	Termination 2	$R_n \rightarrow P_{n-1}$	$r = k_{T2}[R_n]$

M: Monomer P_i^*: Active intermediate with polymerization degree *i*

I: Initiator P_i: Dead polymer with polymerization degree *i*

R_i: Monomer coordinated complex with polymerization degree *i*.

The number of parameters was reduced from ten to five by introducing the quasi-steady state assumption for the concentration of R_i. The simplified kinetic model is shown below:

Initiation		$I + 2M \rightarrow P_1^*$	$r_i = k_{I1}[I][M]^2/(k_{I2}+[M])$
Propagation		$P_n^* + M \rightarrow P_{n+1}^*$	$r_p = k_P[P_n^*][M]$
Termination	Termination 1	$P_n^* \rightarrow P_n$	$r_t = k_{t1}[P^*]$
	Termination 2	$P_n^* + M \rightarrow P_n$	$r_t = k_{t2}[P^*][M]$

Ordinary differential equations for parameter fitting were derived from the above model using the method of Carvalho [26]. The calculation cost was reduced by introducing supporting variables X_i and Y_i. All experimentally obtainable variables, the monomer concentration, the number averaged molecular weight M_n, and the weight averaged molecular weight M_w, were included in the equations as follows:

$$X_i = \sum_{n=1}^{\infty} n^i([P_n^*] + [P_n])$$

$$Y_i = \sum_{n=1}^{\infty} n^i [\mathrm{P}_n^*]$$

$$\frac{\mathrm{d}[\mathrm{I}]}{\mathrm{d}t} = -\frac{\mathrm{d}X_0}{\mathrm{d}t} = -r_\mathrm{i}$$

$$\frac{\mathrm{d}[\mathrm{M}]}{\mathrm{d}t} = -r_\mathrm{p} - r_\mathrm{t2} - r_\mathrm{i}$$

$$\frac{\mathrm{d}[\mathrm{P}^*]}{\mathrm{d}t} = \frac{\mathrm{d}Y_0}{\mathrm{d}t} = r_\mathrm{i} - r_\mathrm{t1} - r_\mathrm{t2}$$

$$\frac{\mathrm{d}Y_1}{\mathrm{d}t} = r_\mathrm{p} + r_\mathrm{i} - k_\mathrm{t1} Y_1 - k_\mathrm{t2}[\mathrm{M}] Y_1$$

$$\frac{\mathrm{d}X_1}{\mathrm{d}t} = r_\mathrm{p} + r_\mathrm{i}$$

$$\frac{\mathrm{d}X_2}{\mathrm{d}t} = 2k_\mathrm{p}[\mathrm{M}] Y_1 + r_i$$

$$M_\mathrm{n} = \frac{X_1}{X_0} M$$

$$M_\mathrm{w} = \frac{X_2}{X_1} M$$

where M indicates the molecular weight of a monomer. Five parameters were simultaneously fitted for minimizing the sum of squared errors of the normalized monomer concentration, M_n, and M_w. Data analysis software IGOR Pro (HULINKS, Tokyo, Japan) was used for fitting. The value of k_i2 always took the negligibly smaller compared with the value of [M] when we fit the five parameters. So we emit k_i2 and recalculated other four parameters all at once.

2.7. Polymerization simulation

The Kinetic Monte Carlo (kMC) method, modified for polymerization simulation [27], was adopted to simulate molecular weight distributions from a reaction model and reaction conditions. The code was written in C++ and run by Visual Studio

2010. The basic algorithm of the kMC method is as follows:

1. Initialize reaction time t as 0

2. Form a list of reaction rates, r_i ($i = 1 \ldots n$), for all possible reactions

3. Calculate R_i for $i = 1 \ldots n$ as $R_{i-1} = \sum_{j=1}^{i} r_j$, where n is the total number of transitions

4. Get a random number u ($0 < u \leq 1$).

5. Find the transition event i that satisfies $R_{i-1} < uR_n \leq R_i$

6. Carry out the event i associated with r_i

7. Obtain a new random number u'

8. Advance t by $\Delta t = R_n^{-1} \ln(1/u')$

9. Update all r_i ($i = 1 \ldots n$) affected by this move

10. Return to 3 until t reaches the total polymerization time.

3. Results and discussion

3.1. Constant temperature polymerization

The results for constant temperature polymerization are shown in Fig. 3. Markers in Fig. 3 show the conversion of the monomer, M_n, and M_w against the reaction time at each temperature and monomer concentration. First, we confirmed the successful termination of the polymerization by peracetic acid. The monomer concentration of the obtained solution did not change after it was maintained at room temperature for days. Peracetic acid solution would instantly deactivate the end group by protonation of the end group. Second, we also confirmed that the viscosity issue was negligible. Obtained absolute viscosity of the polymer solution was only 32.6 mPa s after 1 h reaction with monomer 14 wt% at 25°C. The polymer solution maintained the fluidity and neither gelation nor adhesion to the wall occurred. The increase in the temperature significantly accelerated the reaction; conversion reached 50% at 30 s at 55 °C and at 3600 s at 0 °C

for the same concentration set (Fig. 3(a) and (f)). On the other hand, M_n and M_w decreased at the higher temperature; the M_n at 55 °C was approximately one tenth of the M_n at 0 °C with the same concentration set. Increasing the monomer concentration increased both the conversion and molecular weight (Fig. 3(a) and (b), (f) and (g)). This supports the reaction model shown in Fig. 1 in which the monomer is involved in initiation and propagation, while it is not involved in termination. The temperature dependence of the polymerization steps can be qualitatively estimated from these results. The termination step should have a greater temperature sensitivity than the propagation step to satisfy the tendency of the molecular weight. The initiation step should have a larger sensitivity than the termination step to make conversion larger with a higher termination reaction rate. The best fit results obtained by the procedure described in section 2.6 are shown in Fig. 3 with lines. The fitted curves represent the experimental data well, indicating the validity of the reaction models. The frequency factor k_0 and activation energy E were determined by the Arrhenius plots shown in Fig. 4 and are listed in Table 1. All E values were in the reasonable range, and the order of each step agreed with the previously discussed temperature dependency, with initiation > termination > propagation.

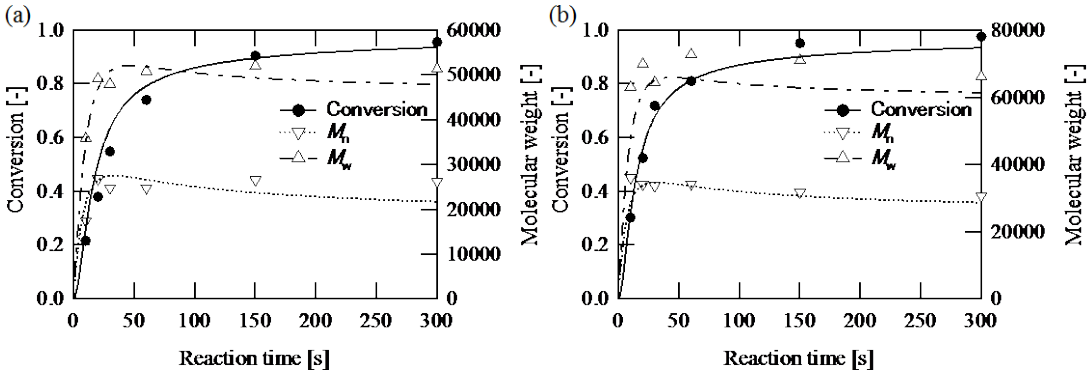

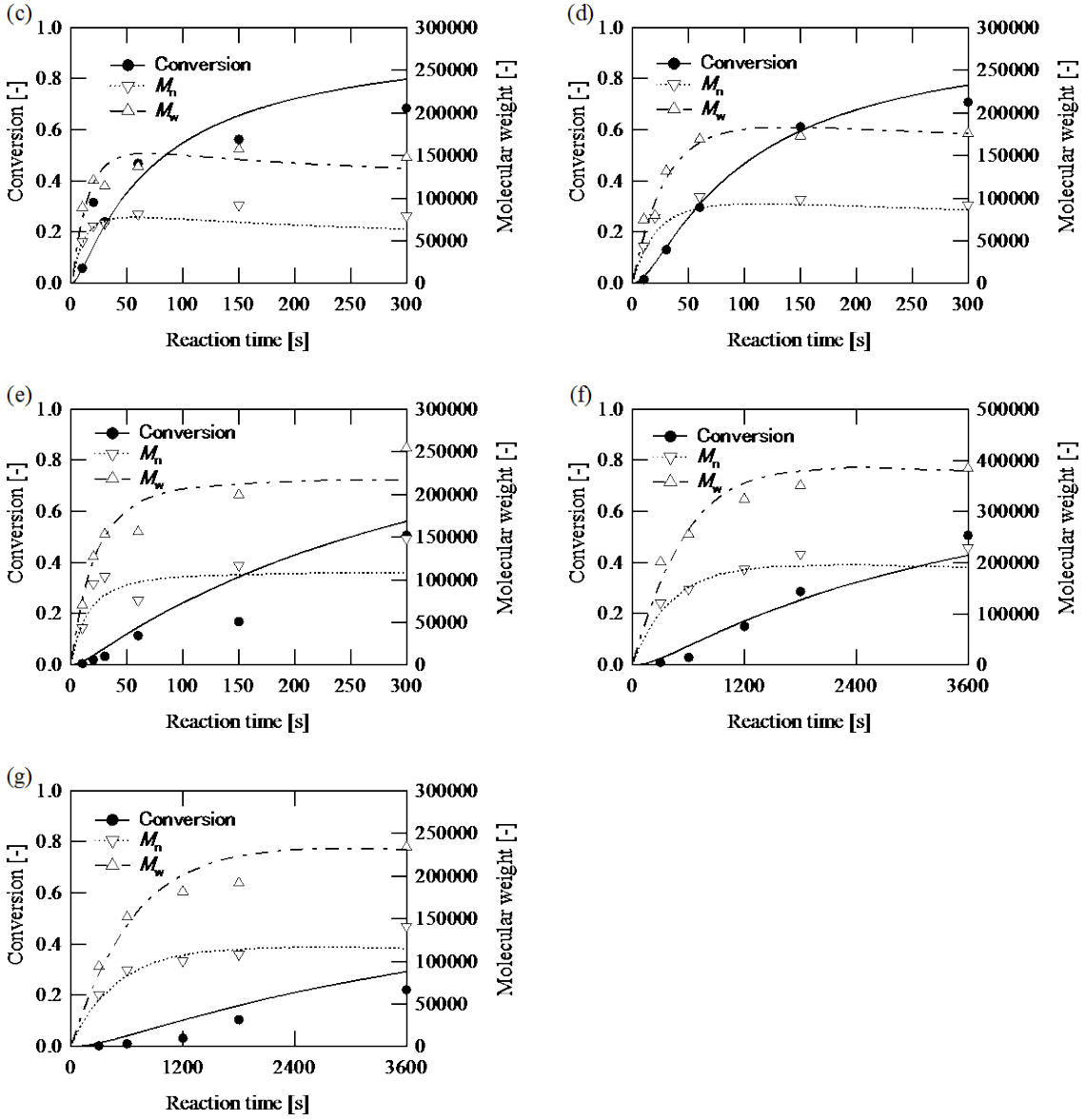

Fig. 3. Reaction results with model fitting: (a) 55˚C, 10 wt%; (b) 55˚C, 15 wt%; (c) 40˚C, 14 wt%; (d) 33˚C, 14 wt%; (e) 25˚C, 14 wt%; (f) 0˚C, 10 wt%; and (g) 0˚C, 5 wt%

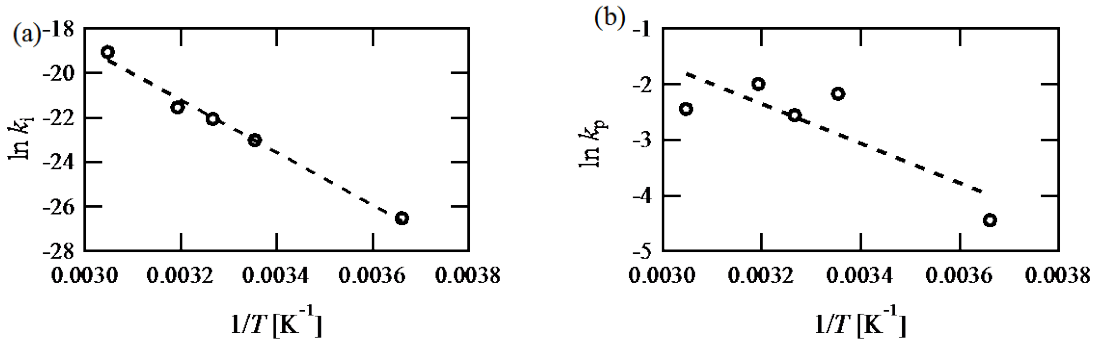

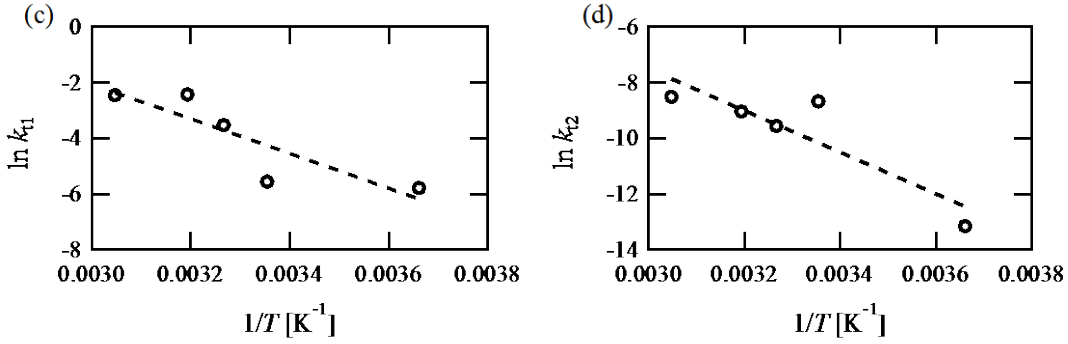

Fig. 4. Arrhenius plots of kinetic parameters: (a) initiation, (b) propagation, (c) termination of a one monomer coordinated Ni complex, and (d) termination of two monomers in a coordinated Ni complex

Table 1 Kinetic constants obtained from Fig. 4.

	k_{i1}	k_p	k_{t1}	k_{t2}
E	98.0 kJ mol^{-1}	29.6 kJ mol^{-1}	51.7 kJ mol^{-1}	62.1 kJ mol^{-1}
k_0	1.48×10^8 m^6 mol^{-2} s^{-1}	8.44×10^3 m^3 mol^{-1} s^{-1}	1.59×10^7 s^{-1}	2.90×10^6 m^3 mol^{-1} s^{-1}

The kinetic model enabled estimation of the concentration profile of active intermediates. Fig. 5 illustrates the estimated concentration of the active intermediate for the experiment at T = 55 °C (monomer 10 wt%), T = 40 °C, (monomer 14 wt%), and T = 25 °C, (monomer 10 wt%). A higher temperature makes the initiation faster and creates a higher number of active intermediates. The peak was around 10 s at T = 55 °C and around 20 s at T = 40 °C. We tried to utilize the estimation by initiating the reaction at the higher temperature and changing the reaction conditions around the peak of the estimated P_n* concentration.

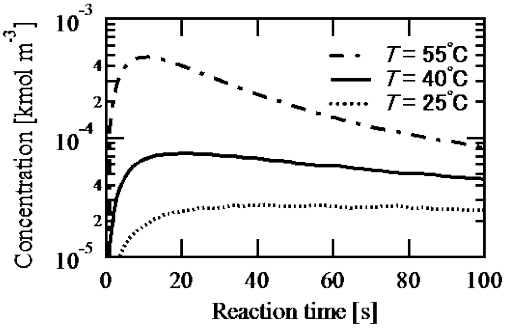

Fig. 5. Concentration profile of P_n* corresponding to (a), (c) and (e) in Fig. 3.

3.2. Block copolymer synthesis

To demonstrate the validity and availability of the estimation, we synthesized a block copolymer. After polymerization of monomer A at 40 °C for 30 s, monomer B was added, and polymerization continued at 25 °C for 15 s. We intended to make a block of monomer B by adding an excess amount of monomer B and by setting the temperature lower after addition so that the deactivation reaction would be suppressed. Fig. 6(a) shows the molecular weight distributions obtained from the designed scheme and control experiment with only the 1st step. The M_n and M_w of the obtained copolymer were 6.6×10^4 and 1.2×10^5, respectively. An apparent shift of the molecular weight from the control was observed, which suggested the sequential growth of the active intermediates generated at the 1st step. Fig. 6(b) indicates the results of GPEC for the obtained polymer in the designed scheme and the homopolymers of monomers A and B. The obtained polymer had three peaks. The small and sharp peak overlapping with monomer A corresponds to the dead polymer generated in the first step. The largest peak around 8 min corresponds to the copolymer, which started polymerization at the first step and continued propagation at the second step. The smallest peak at the position with a slightly longer retention time

than the homopolymer of monomer B would correspond to the copolymer that began polymerization during the second step. The composition would reflect the monomer concentration at the second step, which consists of a high level of monomer B and a minor level of monomer A that was not consumed in the 1st step. To validate the estimated profile of active intermediates, we conducted the block copolymer synthesis with twice the residence time and half the flow rate. Table 2 compares the conditions and conversion of each monomer species. By increasing the residence time, the conversion of monomer A naturally increased, but the conversion of monomer B decreased. This tendency can be attributed to the deactivation of the active species during the extended residence time at the 1st step and supports the estimated concentration value of active intermediates, which was decreased in the control scheme.

Based on these pieces of evidence, we can conclude that the estimated profile of active intermediates was valid and we successfully synthesized a block copolymer.

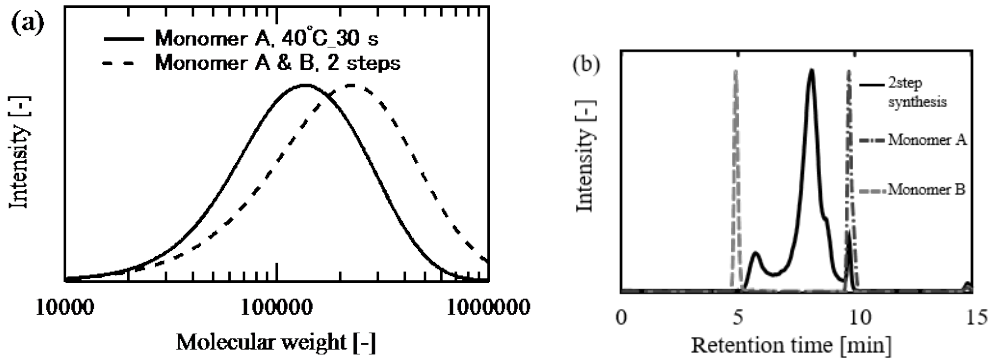

Fig. 6. (a) Molecular weight distribution and (b) GPEC profile of the obtained copolymer

Table 2 Comparison of conversion with different residence times

Residence time (1st	Conversion	of	Conversion	of	Estimated	P_n*

step- 2nd step) [s]	monomer A	monomer B	concentration after the 1st step [M]
30-15 (designed scheme)	0.208	0.083	7.1×10^{-5}
60-30 (control scheme)	0.434	0.072	5.8×10^{-5}

3.3 Homopolymer synthesis with temperature jump

To synthesize a polymer with a monodispersed molecular weight distribution, it is effective to make the initiation reaction faster than the propagation reaction and to make the termination reaction slower than the other reactions. A higher temperature can boost the initiation reaction, and a lower temperature can efficiently suppress the initiation and termination reactions. We designed the temperature jumping operation for conducting the initiation reaction at the high temperature, 60 °C, and the propagation reaction at the lower temperature, 0 °C. The concentrations of monomer and initiator were fixed at 20 wt% and 0.033 M, respectively. The residence time at 60 °C was designed based on the kMC simulation. Fig. 7 summarizes the results of the simulation with the kinetic parameters in Table 1. In the case of the constant temperature operation at 60 °C, the value of M_w/M_n increased almost linearly against the conversion by the simultaneous initiation, propagation and termination reactions. The temperature change had a significant impact on the profile. The M_w/M_n decreased after cooling because the active intermediates generated in the high temperature zone uniformly propagated and terminated. Then, the M_w/M_n increased again with the conversion. This is attributed to the new active

intermediates generated in the low temperature zone. Rapid cooling after 0.1 s of reaction at 60 °C enabled a surprisingly small M_w/M_n, around 1.05, in the minuscule conversion region. The 1.0 s reaction in the high temperature zone enabled the more stable M_w/M_n curve, although the dead polymer that formed within 1.0 s increased the M_w/M_n. Then, 0.5 s was determined to be the optimal residence time for the high temperature zone.

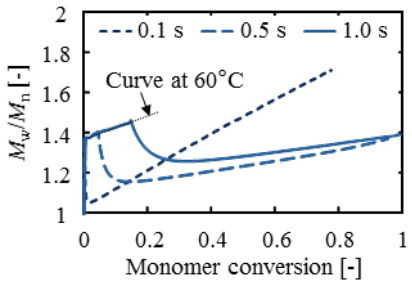

Fig. 7. Simulated M_w/M_n profiles in the case of the temperature jumping operation. The legend shows the residence time in the high temperature zone.

Fig. 8 shows the molecular weight distribution obtained by the designed scheme and constant temperature operation with the same concentration set. The designed scheme successfully resulted in a sharp peak owing to the uniform propagation of active intermediates generated at the high temperature. Table 3 summarizes the experimental and simulation outputs for the designed system and control experiments. The designed scheme showed much higher conversion than the simple summation of 0 °C, 30 s and 60 °C, 0.5 s. However, both the conversion and M_w/M_n of the experimental results were worse than those of the simulated values. The most likely reason was the effect of ethyl acetate, which was essential for reducing the molecular weight and preventing clogging, but it was not included in the kinetic model.

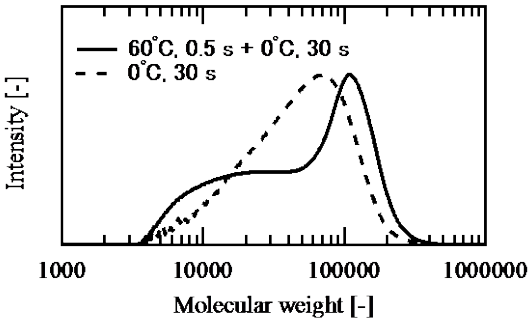

Fig. 8. Molecular weight distributions of the polymers synthesized in the temperature jumping operation from 60 °C to 0 °C and the constant temperature operation at 0 °C

Table 3 Output of various schemes: monomer 20 wt%, initiator 0.033 M, and [M]/[I] = 30/1

	conversion [-]	M_w/M_n	M_n
60 °C, 0.5 s	0.09	2.07	17909
0 °C, 30 s	0.04	1.62	59792
designed scheme	0.28	1.71	72557
designed scheme (simulation)	0.38	1.21	65980

4. Conclusions

The micro flow reactor was successfully applied to the rate analysis of polymerization by allowing for a short reaction time and rigid temperature control. The validity and utility of the kinetic analysis were demonstrated by synthesizing a block copolymer with a non-living polymerization system. The temperature jumping operation, 0.5 s initialization at high temperature followed by 30 s growth at low temperature, was examined based on the estimated kinetic model. Although the experimental results were

worse than the simulation for the M_w/M_n and conversion, the sharpness values of the molecular weight distribution and productivity were improved from the constant temperature operation. Therefore, a micro flow reactor system supported by reliable kinetic information would be an ideal tool to improve both the productivity and quality of highly functionalized polymers.

Acknowledgments

We gratefully acknowledge the financial support provided by “the Japan Society for the Promotion of Science” (JSPS), grant numbers 25220913 and 15J00287.

References

[1] S. Schwolow, A. Neumüller, L. Abahmane, N. Kockmann, T. Röder, Design and application of a millistructured heat exchanger reactor for an energy-efficient process, Chem. Eng. Process. Process Intensif. 108 (2016) 109–116. doi:10.1016/j.cep.2016.07.017.

[2] F. Kaske, S. Dick, S.A. Pajoohi, D.W. Agar, The influence of operating conditions on the mass transfer performance of a micro capillary contactor with liquid-liquid slug flow, Chem. Eng. Process. Process Intensif. 108 (2016) 10–16. doi:10.1016/j.cep.2016.06.010.

[3] R.L. Hartman, J.P. McMullen, K.F. Jensen, Deciding whether to go with the flow: evaluating the merits of flow reactors for synthesis., Angew. Chem. Int. Ed. Engl. 50 (2011) 7502–7519. doi:10.1002/anie.201004637.

[4] K. Mae, Advanced chemical processing using microspace, Chem. Eng. Sci. 62 (2007) 4842–4851. doi:10.1016/j.ces.2007.01.012.

[5] S. Marre, J. Park, J. Rempel, J. Guan, M.G. Bawendi, K.F. Jensen, Supercritical continuous-microflow synthesis of narrow size distribution quantum dots, Adv. Mater. 20 (2008) 4830–4834. doi:10.1002/adma.200801579.

[6] A. Nagaki, K. Imai, H. Kim, J. Yoshida, Flash synthesis of TAC-101 and its analogues from 1,3,5-tribromobenzene using integrated flow microreactor systems, RSC Adv. 1 (2011) 758–760. doi:10.1039/C1RA00377A.

[7] S. Watanabe, S. Ohsaki, T. Hanafusa, K. Takada, H. Tanaka, K. Mae, et al., Synthesis of zeolitic imidazolate framework-8 particles of controlled sizes, shapes, and gate adsorption characteristics using a central collision-type microreactor, Chem. Eng. J. 313 (2017) 724–733. doi:10.1016/j.cej.2016.12.118.

[8] S. Marre, K.F. Jensen, Synthesis of micro and nanostructures in microfluidic systems, Chem. Soc. Rev. 39 (2010) 1183–1202. doi:10.1039/b821324k.

[9] D.M. Roberge, L. Ducry, N. Bieler, P. Cretton, B. Zimmermann, Microreactor technology: A revolution for the fine chemical and pharmaceutical industries?, Chem. Eng. Technol. 28 (2005) 318–323. doi:10.1002/ceat.200407128.

[10] A. Adamo, R.L. Beingessner, M. Behnam, J. Chen, T.F. Jamison, K.F. Jensen, et al.,

On-demand continuous-flow production of pharmaceuticals in a compact, reconfigurable system, Science (80-.). 352 (2016) 61–67. doi:10.1126/science.aaf1337.

[11] T. Tsubogo, H. Oyamada, S. Kobayashi, Multistep continuous-flow synthesis of (R)- and (S)-rolipram using heterogeneous catalysts, Nature. 520 (2015) 329–332. doi:10.1038/nature14343.

[12] M. Furuta, K. Mukai, D. Cork, K. Mae, Continuous crystallization using a sonicated tubular system for controlling particle size in an API manufacturing process, Chem. Eng. Process. Process Intensif. 102 (2016) 210–218. doi:10.1016/j.cep.2016.02.002.

[13] F. Bally, C. a. Serra, V. Hessel, G. Hadziioannou, Homogeneous polymerization: Benefits brought by microprocess technologies to the synthesis and production of polymers, Macromol. React. Eng. 4 (2010) 543–561. doi:10.1002/mren.201000006.

[14] L.S. Méndez-Portillo, C. Dubois, P. a. Tanguy, Free-radical polymerization of styrene using a split-and-recombination (SAR) and multilamination microreactors, Chem. Eng. J. 256 (2014) 212–221. doi:10.1016/j.cej.2014.05.134.

[15] A. Nagaki, T. Iwasaki, K. Kawamura, D. Yamada, S. Suga, T. Ando, et al., Microflow system controlled carbocationic polymerization of vinyl ethers, Chem. - An Asian J. 3 (2008) 1558–1567. doi:10.1002/asia.200800081.

[16] A. Kumar, J. Hasan, A. Majji, A. Avhale, S. Gopinathan, P. Sharma, et al., Continuous-

Flow Synthesis of Regioregular Poly(3-Hexylthiophene): Ultrafast Polymerization with High Throughput and Low Polydispersity Index, J. Flow Chem. 4 (2014) 206–210. doi:10.1556/JFC-D-14-00009.

[17] C.G. Dobie, K.V.K. Boodhoo, Surfactant-free emulsion polymerisation of methyl methacrylate and methyl acrylate using intensified processing methods, Chem. Eng. Process. Process Intensif. 49 (2010) 901–911. doi:10.1016/j.cep.2010.08.005.

[18] J. Vandenbergh, T. Tura, E. Baeten, T. Junkers, Polymer end group modifications and polymer conjugations via “click” chemistry employing microreactor technology, J. Polym. Sci. Part A Polym. Chem. 52 (2014) 1263–1274. doi:10.1002/pola.27112.

[19] F. a. Leibfarth, J. a. Johnson, T.F. Jamison, Scalable synthesis of sequence-defined, unimolecular macromolecules by Flow-IEG, Proc. Natl. Acad. Sci. 112 (2015) 10617–10622. doi:10.1073/pnas.1508599112.

[20] J. Yoshida, Y. Takahashi, A. Nagaki, Flash chemistry: flow chemistry that cannot be done in batch, Chem. Commun. 49 (2013) 9896–9904. doi:10.1039/C3CC44709J.

[21] S. Asano, T. Maki, K. Mae, Evaluation of mixing profiles for a new micromixer design strategy, AIChE J. 57 (2015) n/a-n/a. doi:10.1002/aic.15082.

[22] B.J. Reizman, K.F. Jensen, Simultaneous solvent screening and reaction optimization in microliter slugs, Chem. Commun. 51 (2015) 2–5. doi:10.1039/C5CC03651H.

[23] D.A. Barnes, G.M. Benedikt, B.L. Goodall, S.S. Huang, H.A. Kalamarides, S. Lenhard, et al., Addition polymerization of norbornene-type monomers using neutral nickel complexes containing fluorinated aryl ligands, Macromolecules. 36 (2003) 2623–2632. doi:10.1021/ma030001m.

[24] M.M. Mandal, C. Serra, Y. Hoarau, K.D.P. Nigam, Numerical modeling of polystyrene synthesis in coiled flow inverter, Microfluid. Nanofluidics. 10 (2011) 415–423. doi:10.1007/s10404-010-0679-z.

[25] S.K. Kurt, M.G. Gelhausen, N. Kockmann, Axial Dispersion and Heat Transfer in a Milli/Microstructured Coiled Flow Inverter for Narrow Residence Time Distribution at Laminar Flow, Chem. Eng. Technol. 1 (2015) 1122–1130. doi:10.1002/ceat.201400515.

[26] A.B. de Carvalho, P.E. Gloor, A.E. Hamielec, A kinetic mathematical model for heterogeneous Ziegler-Natta copolymerization, Polymer (Guildf). 30 (1989) 280–296. doi:10.1016/0032-3861(89)90118-3.

[27] P.H.M. Van Steenberge, D.R. D'hooge, M.F. Reyniers, G.B. Marin, Improved kinetic Monte Carlo simulation of chemical composition-chain length distributions in polymerization processes, Chem. Eng. Sci. 110 (2014) 185–199. doi:10.1016/j.ces.2014.01.019.